

Research Paper

# Basic Transcription Factor 3 (BTF3) Regulates Transcription of Tumor-Associated Genes in Pancreatic Cancer Cells

Grace Kusumawidjaja<sup>1,†</sup>

Hany Kayed<sup>1,†</sup>

Nathalia Giese<sup>1</sup>

Andrea Bauer<sup>2</sup>

Mert Erkan<sup>1</sup>

Thomas Giese<sup>3</sup>

Jörg D. Hoheisel<sup>2</sup>

Helmut Friess<sup>1</sup>

Jörg Kleeff<sup>1,\*</sup>

<sup>1</sup>Department of General Surgery; University of Heidelberg; Heidelberg, Germany

<sup>2</sup>Division of Functional Genome Analysis; German Cancer Research Center; Heidelberg, Germany

<sup>3</sup>Institute of Immunology; University of Heidelberg; Heidelberg, Germany

<sup>†</sup>These authors contributed equally to this study.

\*Correspondence to: Jörg Kleeff; Department of General Surgery; University of Heidelberg; Im Neuenheimer Feld 110; Heidelberg 69120 Germany; Tel.: +49.6221.56.4860; Fax: +49.6221.56.6903; Email: joerg\_kleeff@med.uni-heidelberg.de

Original manuscript submitted: 11/21/06

Manuscript accepted: 12/13/06

Previously published online as a *Cancer Biology & Therapy* E-publication: <http://www.landesbioscience.com/journals/cc/abstract.php?id=3704>

## KEY WORDS

BTF3, EPHB2, pancreatic cancer, chemotherapy, radiotherapy, apoptosis, microarray

## ABSTRACT

Basic transcription factor 3 (BTF3) acts as a transcription factor and modulator of apoptosis, and is differentially expressed in colorectal cancer and glioblastomas. In the present study, the expression of BTF3, as well as its role in apoptosis and gene transcription, was analyzed in pancreatic ductal adenocarcinoma (PDAC). QRT-PCR, immunohistochemistry, immunoblotting, and immunofluorescence analyses were carried out to investigate BTF3 mRNA/protein expression and localization. BTF3 silencing in pancreatic cancer cells was performed using specific siRNA molecules. Functional analyses were carried out using cell growth assays, apoptosis assays, and DNA array analysis. BTF3 and BTF3a exhibited 1.3-fold and 4.6-fold increased median mRNA levels in PDAC tissues, compared to normal pancreatic tissues. BTF3 localized mainly in the cytoplasm and nuclei of tubular complexes and pancreatic cancer cells. Pancreatic cancer cell lines expressed the mRNA and protein of BTF3a (27 kDa) and BTF3b (22 kDa) isoforms. BTF3 silencing using specific siRNA molecules did not influence apoptosis induced by chemotherapy or radiotherapy. In contrast, BTF3 silencing resulted in down-regulation of several cancer-associated genes, including EPHB2, ABL2, HPSE2 and ATM, and up-regulation of KRAG, RRAS2, NFκ-B, MRV11, MADCAM1 and others. In conclusion, BTF3 is overexpressed in PDAC, where it acts as a transcriptional regulator rather than a direct modulator of apoptosis.

## INTRODUCTION

Basic transcription factor 3 (BTF3), also known as nascent polypeptide-associated complex β (NACB), is a 27 KD protein<sup>1,2</sup> that is involved in the initiation of transcription by RNA polymerase from proximal promoter elements such as the TATA box and CAAT box sequences.<sup>1,3,4</sup> BTF3 is present in two isoforms: BTF3a, which has the transcription characteristics of BTF3, and BTF3b, which lacks the first 44 amino acids of BTF3a and is transcriptionally inactive.<sup>4,5</sup> BTF3 is also able to inhibit the transcription of genes such as GAL, which acts as a paracrine regulator of prolactin expression.<sup>6</sup> BTF3 loss-of-function mutation in mice leads to death in the early stages of development,<sup>7</sup> pointing to an important role of this gene during normal development. In addition to its function as a transcriptional regulator, BTF3 is also involved in cell cycle regulation and apoptosis.<sup>8-10</sup> For example, altered BTF3 expression is associated with apoptosis in BL60 Burkitt lymphoma cells,<sup>9</sup> and down-regulation of BTF3 is involved in inhibition of transcription and protein synthesis in apoptotic K562 cells.<sup>11</sup>

In cancer, BTF3 is found to be overexpressed in glioblastoma multiforme<sup>12</sup> and sporadic colorectal cancer.<sup>13</sup> We have previously identified BTF3 as a differentially expressed gene in PDAC and chronic pancreatitis (CP).<sup>14,15</sup> In the present study we: (1) analyzed the expression of BTF3 mRNA and protein in the normal and diseased pancreas (CP and PDAC) and pancreatic cancer cell lines, and the localization of BTF3 in these tissues; (2) analyzed the functional consequences of BTF3 silencing in pancreatic cancer cell lines in terms of resistance to chemo/radiotherapy-induced apoptosis, and (3) used a DNA micro-array analysis to identify regulation of genes after BTF3 silencing, in order to specify the role of BTF3 in the transcriptional regulation of tumor-associated genes.

## MATERIALS AND METHODS

**Tissue samples.** PDAC (n = 46) and CP (n = 10) tissue specimens were obtained from patients with a median age of 71 years (range: 38–83 years) in whom pancreatic resections were performed. Normal human pancreatic tissue samples (n = 29) were

obtained through an organ donor program from previously healthy individuals. All samples were confirmed by histological analysis. Freshly removed tissues (within 5 min after surgical excision) were: (a) fixed in paraformaldehyde solution for 12 to 24 h and then paraffin embedded for histological analysis; (b) kept in RNAlater (Ambion Ltd., Huntingdon, Cambridgeshire, UK) for RNA analysis, or (c) snap-frozen in liquid nitrogen and maintained at  $-80^{\circ}\text{C}$  for protein analysis. The Human Ethics Committee of the University of Heidelberg, Germany, and the University of Bern, Switzerland, approved all studies, and written informed consent was obtained from all patients.

**Cell culture and induction of apoptosis.** Pancreatic cancer cell lines were grown routinely in RPMI medium (Aspc-1, BxPc-3, Capan-1, Colo-357, SU8686 and T3M4) or DMEM medium (MiaPaCa-2 and Panc-1), supplemented with 10% FCS and 100 U/ml penicillin (complete medium), and incubated in a 5%  $\text{CO}_2$  humidified atmosphere. For induction of apoptosis, cells were exposed to 5-FU or gemcitabine at the indicated doses. Irradiation was performed using a 137 Cs  $\gamma$ -irradiator at 7.5 Gy/min for 2 min, delivering a total dose of 15 Gy.

**Real-time quantitative polymerase chain reaction (QRT-PCR).** All reagents and equipment for mRNA/cDNA preparation were supplied by Roche Applied Science (Mannheim, Germany). mRNA was prepared by automated isolation using the MagNA pure LC instrument and isolation kit I (for cells) and kit II (for tissues). cDNA was prepared using the first strand cDNA synthesis kit for RT-PCR (AMV) according to the manufacturer's instructions. Real-time PCR was performed using the LightCycler FastStart DNA SYBR Green kit. The primer sequences for BTF3 and BTF3a and EPHB2 were obtained from Search-LC (Heidelberg, Germany). The primer sequences for BTF3 amplification were: 5' TCT CCT TAA AGA AGT TAG GGG TAA ACA; 3' CGG CCA GTC TCC TTA AAC TAG TCA, and for BTF3a: 5' GGA GAG GAA GGC GAT GCG ACG GAC; 3' TTC CTT TCC CAC CAA TGC GCA CTT GTG. The BTF3 primers amplified both isoforms (BTF3a and BTF3b), whereas the BTF3a primers were specific only for the BTF3a isoform. The number of specific transcripts was normalized to housekeeping genes (cyclophilin B and HPRT). The data of the two independent analyses for each sample and parameter were averaged and presented as adjusted transcripts/ $\mu\text{l}$  cDNA.<sup>16,17</sup>

**Immunohistochemistry.** Paraffin-embedded tissue sections (2–3  $\mu\text{m}$  thick) were immunostained using the DAKO Envision TM+ system (DAKO Corporation, Carpinteria, CA). Tissue sections were de-paraffinized in xylene and rehydrated in progressively decreasing concentrations of ethanol. Thereafter, the slides were placed in washing buffer (10 mM Tris-HCl, 0.85% NaCl, 0.1% bovine serum albumin, pH 7.4). After antigens were retrieved by boiling the tissue sections in 10 mM citrate buffer for 20 min in the microwave oven, consecutive sections were incubated with rabbit polyclonal BTF3a/b antibodies (Zymed Laboratories, Inc., Karlsruhe, Germany), goat polyclonal EPHB2 antibodies (R&D systems, Wiesbaden-Nordenstadt, Germany),<sup>18</sup> or normal rabbit or goat IgG (DAKO) as negative controls in an antibody diluent with background-reducing components (DAKO) at  $4^{\circ}\text{C}$  overnight. For BTF3 and EPHB2 detection, the slides were incubated with HRPO-conjugated anti-rabbit IgG (Amersham International, Buckinghamshire, UK) and anti-goat IgG (Invitrogen GmbH, Karlsruhe, Germany), respectively, for 1 h at room temperature. DAB-chromogen/ $\text{H}_2\text{O}_2$  substrate mixture (DAKO) was applied to tissue sections, and then slides were counterstained with Mayer's hematoxylin. Sections were washed, dehydrated in

progressively increasing concentrations of ethanol, and mounted with xylene-based mounting medium. Slides were analyzed using the Axioplan 2 imaging microscope (Carl Zeiss Light Microscope, Göttingen, Germany).

**Immunofluorescence.** Cells were washed three times with PBS and fixed in 4% paraformaldehyde for 20 min, followed by 5 min incubation in 30 mM glycine/PBS to quench the effect of paraformaldehyde. Cells were washed in PBS-T (0.05% Tween 20 in PBS pH 7.4) and blocked with PBS containing 3% bovine serum albumin (KPL, Gaithersburg, MD) for 1 h, followed by incubation with polyclonal rabbit BTF3a/b antibodies (Zymed Laboratories, Inc.) for 1 h. Cells were washed in PBS-T and incubated with FITC-labeled anti-rabbit IgG for 1 h. All incubation steps were carried out at room temperature. Next, cells were washed and their nuclei were counterstained with DAPI (1 mg/ml PBS, pH 7.4). Microscopic analysis was carried out using the Spectral Confocal Microscope Leica TCS SL (Leica Microsystems GmbH, Heidelberg, Germany).

**Immunoblotting.** Cells were washed twice with ice-cold PBS and lysed with lysis buffer (50 mM Tris-HCl, 100 mM NaCl, 2 mM EDTA, 1% SDS) containing one tablet of complete mini-EDTA-free protease inhibitor cocktail (Roche Applied Science). Protein concentration was determined by the BCA protein assay (Pierce Chemical Co., Rockford, IL). Cell lysates (20  $\mu\text{g}$ /lane) were separated on SDS-polyacrylamide gels and electroblotted onto nitrocellulose membranes. Membranes were then incubated in blocking solution (5% nonfat milk in 20 mM Tris-HCl, 150 mM NaCl, 0.1% Tween-20), followed by incubation with rabbit polyclonal BTF3a/b antibodies (Zymed Laboratories, Inc.) at  $4^{\circ}\text{C}$  overnight. The membranes were then washed and incubated with donkey anti-rabbit HRPO-conjugated IgG (Amersham International) for 1 h at room temperature. Equal loading and transfer were confirmed using  $\gamma$ -tubulin antibodies (Santa Cruz Biotechnology, Inc.). Antibody detection was performed by an enhanced chemiluminescence reaction (Amersham International).

**siRNA transfection.** For siRNA silencing, Aspc-1 and Capan-1 and Panc-1 cells were plated in 6-well plates at a density of  $2 \times 10^5$  cells per well for 24 h. In vitro transfection was performed using RNAifect transfection reagent (Quiagen, Hilden, Germany) according to the manufacturer's instructions. The cells were transfected with 5  $\mu\text{g}$  siRNA BTF3-specific sense 5'GGA UGA UGA UGA UGA AGU Utt 3', antisense 5'AAC UUC AUC AUC AUC AUC Ctc 3'(Ambion, Inc. Austin, TX) and control siRNA: aat tct ccg aac gtg tca cgt (Quiagen, Hilden, Germany) for the indicated time (24 and 48 h).

**Cell proliferation assay.** The 3-(4,5-dimethyl-thiazol-2-yl)-2-5-diphenyltetrazolium-bromide (MTT) (Sigma Aldrich, St. Louis, MO) assay was used to assess cell proliferation.<sup>19</sup> Cells were seeded in 96-well plates at a density of  $5 \times 10^3$  cells/well overnight, and then treated with the indicated doses of 5-FU or gemcitabine for 48 h. MTT (5mg/ml in PBS pH 7.4) was added to a final concentration of 0.5 mg/ml. After 4 h of incubation, the formazan products were solubilized with acidic isopropanol and the optical density was measured at 570 nm. The absorbance was corrected for blank readings. The experiments were carried out in triplicate and repeated three times.

**Cell cycle analysis.** Both adherent and suspended Aspc-1 and Capan-1 cells were collected for analysis after treatment with 5  $\mu\text{M}$  5-FU, 50 ng/ml gemcitabine or 15 Gy irradiation. Cell cycle analysis was performed using a Nicoletti hypotonic fluorochrome solution (propidium iodide 50  $\mu\text{g}$ /ml, sodium citrate 0.1%, Triton X-100 0.1%). Flow cytometry was performed with a FACS instrument (Becton Dickinson Biosciences, Erembodegem, Belgium).

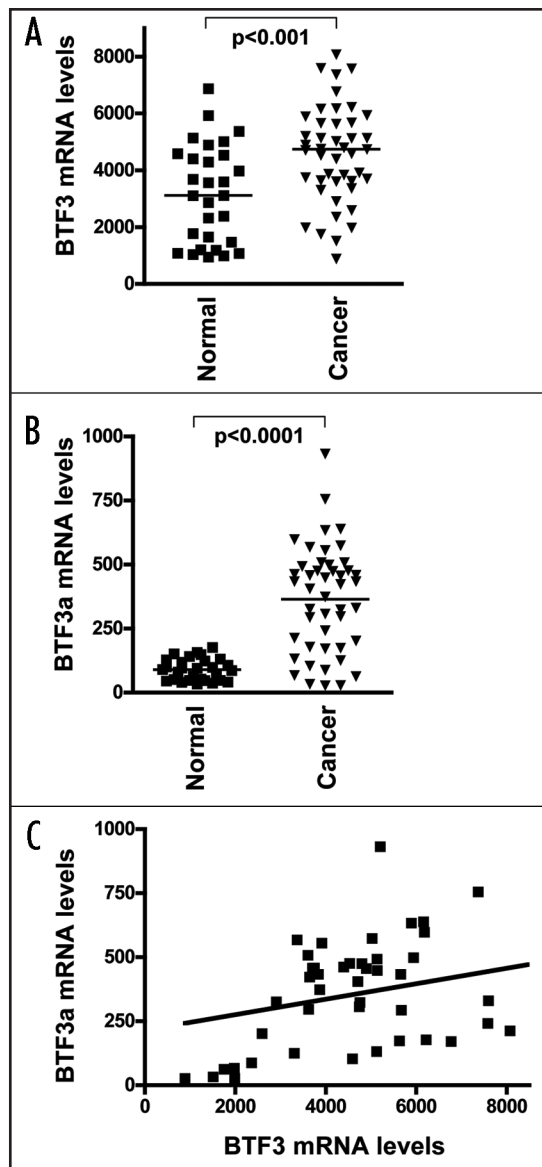


**Figure 1.** mRNA expression levels of BTF3 and BTF3a in pancreatic tissues. Real-time quantitative RT-PCR analysis of mRNA levels for total BTF3 (A) and BTF3a (B) in normal (squares) and PDAC (triangles) tissue samples was performed as described in the Methods section. Horizontal lines represent the median mRNA levels. (C) Correlation between total BTF3 and BTF3a in PDAC tissues: total BTF3 mRNA expression levels directly correlate with the mRNA levels of BTF3a in PDAC cases. Values on x and y axes represent mRNA values in copy number/ $\mu$ l cDNA. RNA input was normalized to the average expression of the two housekeeping genes HPRT and cyclophilin B, and is presented as copy number/ $\mu$ l cDNA.

**Detection of apoptosis.** Detection of apoptosis was carried out by the Annexin-V-Fluos kit (Roche Diagnostics). Both adherent and floating cells were collected for analysis after treatment with chemotherapy or irradiation. Cells were collected by centrifugation at 200 g for 5 min. Subsequently the cell pellet was resuspended in 100  $\mu$ l Annexin-V-Fluos in a HEPES buffer (10 mM HEPES/NaOH, pH 7.4, 140 mM sodium chloride, 5 mM calcium chloride) containing propidium iodide, and incubated for 10–15 min. Subsequently, flow cytometry was performed with a FACS instrument (Becton Dickinson Biosciences).

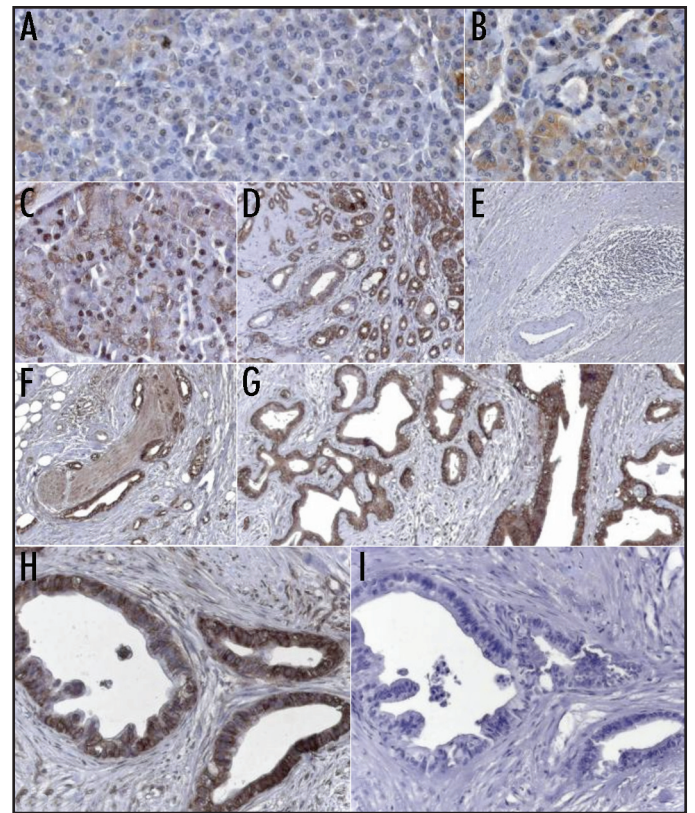


**Figure 2.** BTF3 localization in human pancreatic tissues. Immunohistochemistry analysis was performed as described in the Methods section. (A and B) Normal pancreatic tissues showing weak to moderate BTF3 staining in the cytoplasm and nuclei of acinar and ductal cells. (C–E) Chronic pancreatitis tissues displaying moderate staining in acinar cells (C), strong BTF3 staining in the cytoplasm of tubular complexes (D), and absent staining in vessels and inflammatory cells (E). (F–I) Pancreatic cancer tissues showing intense staining of BTF3 in the cytoplasm and nuclei of cancer cells (F–H), as well as in enlarged nerves (F). Note the absent staining in a consecutive tissue section incubated with normal rabbit IgG as a negative control (H and I).

**DNA microarrays.** Human cDNAs representing 3500 different human genes, which were selected due to their previously identified role in PDAC,<sup>20</sup> were PCR-amplified using amino-modified M13 universal primers. PCR products were purified with PCR multi-screen columns (Millipore GmbH, Schwalbach, Germany), suspended in spotting solution (TeleChem International Inc., Sunnyvale, CA) and arrayed onto slides with an epoxy surface (Epoxy Slides, Quantifoil Micro Tools GmbH, Jena, Germany). DNA spotting was performed with a Micro-Arrayer from Engineering Services Inc. (Virtek's arrayer system, BioRad, Munich, Germany) using SMP3 pins (TeleChem International Inc., Sunnyvale, CA). Each microarray presents 3872 spots divided into 16 blocks, containing each spot in duplicate.

**Transcriptional profiling.** Total RNA was extracted with the guanidine isothiocyanate method<sup>21</sup> from BTF3 siRNA-silenced ASPC1, Capan-1 and Panc-1 cells as well as control siRNA-transfected cells. Total RNA extracted from MiaPaCa-2 pancreatic cancer cells was used as a reference control. Fluorescence-labeled cDNA samples were prepared from 10  $\mu$ g total RNA with incorporation of Cy3- or Cy5-labeled dCTP during first-strand synthesis. The labeling reaction was performed at least three times in total. Hybridization was done in SlideHyb-Buffer 1 (Ambion Inc., Austin, TX) under glass coverslips at 62°C overnight. To prevent bias caused by

preferential label incorporation into particular sequences, the dyes were swapped between hybridizations. After washing in 0.1 x sodium saline citrate for 3 min and drying using nitrogen, fluorescence signals were detected on a confocal ScanArray 5000 scanner (Packard BioChip Technologies, Billerica, MA). Quantification of the signal intensities was performed with the GenePix Pro 4.1 software (Axon Instruments, Inc., Union City, CA).

**Data analysis.** Data quality assessment, normalization and correspondence cluster analysis were performed with the analysis and data warehouse software package M-CHiPS (Multi-Conditional Hybridization Intensity Processing System), in which more than 7800 hybridization experiments are currently stored (<http://www.mchips.org>).<sup>22,23</sup> Normalization was performed as described in detail by Beissbarth et al.<sup>24</sup> For further analysis, only genes that exhibited significant changes between at least one sample and the control material were selected. Data analysis and also the compilation of experimental and sample-specific annotations met the criteria for MIAME2 compliance.<sup>25</sup> Correspondence analysis<sup>22,23</sup> is an explorative computational method for the study of associations between variables. Much like principle component analysis, it displays a low-dimensional projection of the data onto a plane. Data are projected simultaneously for two variables, such as genes and patient samples, thus revealing associations between them. The closer the data points are located on the blot, the higher the degree of correspondence, thereby enabling superior data interpretation.

**Statistical analysis.** Results are expressed as the mean  $\pm$  standard error of the mean (SEM) unless indicated otherwise. For statistical analysis the non-parametric Mann-Whitney and Spearman-Rho tests were used, and significance was defined as  $p < 0.05$ . Graphs were generated using GraphPad prism2 software (GraphPad Software, San Diego, CA).

## RESULTS

**BTF3 and BTF3a mRNA levels in PDAC tissues.** To confirm previous DNA microarray data<sup>14</sup> and to exactly quantify the mRNA levels of BTF3 and BTF3a, qRT-PCR was carried out. The BTF3 primers detect both isoforms (BTF3a and BTF3b), whereas the BTF3a primers are only specific for the BTF3a isoform. BTF3b expression levels can therefore be estimated indirectly by subtracting BTF3a from BTF3 levels. This analysis demonstrated 1.3-fold increased median total BTF3 mRNA levels in PDAC ( $n = 46$ ) tissues compared to the normal pancreas ( $n = 29$ ) ( $p < 0.001$ ) (Fig. 1A). Specifically, the median total BTF3 mRNA expression was 4746 (range: 884–16160) copies/ $\mu$ l cDNA in PDAC tissues. In normal pancreatic tissues, the median total BTF3 mRNA was 3115 (range: 952–6875) copies/ $\mu$ l cDNA. More prominently, median BTF3a mRNA expression levels were 4.6-fold higher in PDAC tissues ( $p < 0.0001$ ) compared to normal pancreatic tissues (Fig. 1B), suggesting that BTF3a is the cancer-specific isoform. To confirm this specificity, the BTF3a/total BTF3 ratio in individual PDAC cases and normal controls was calculated. The median BTF3a/total BTF3 ratio was 0.07 (range: 0.01–0.14) in PDAC cases and 0.03 (range: 0.02–0.06) in normal controls. Thus median BTF3a mRNA expression was 414 (range: 27–932) copies/ $\mu$ l cDNA in PDAC tissues. In normal pancreatic tissues, the median BTF3a mRNA was 90 (range: 34–176) copies/ $\mu$ l cDNA. Correlation analysis between total BTF3 and BTF3a mRNA levels in PDAC cases revealed a significant direct correlation ( $p < 0.005$ , Spearman  $r$  0.4215, 95% confidence interval

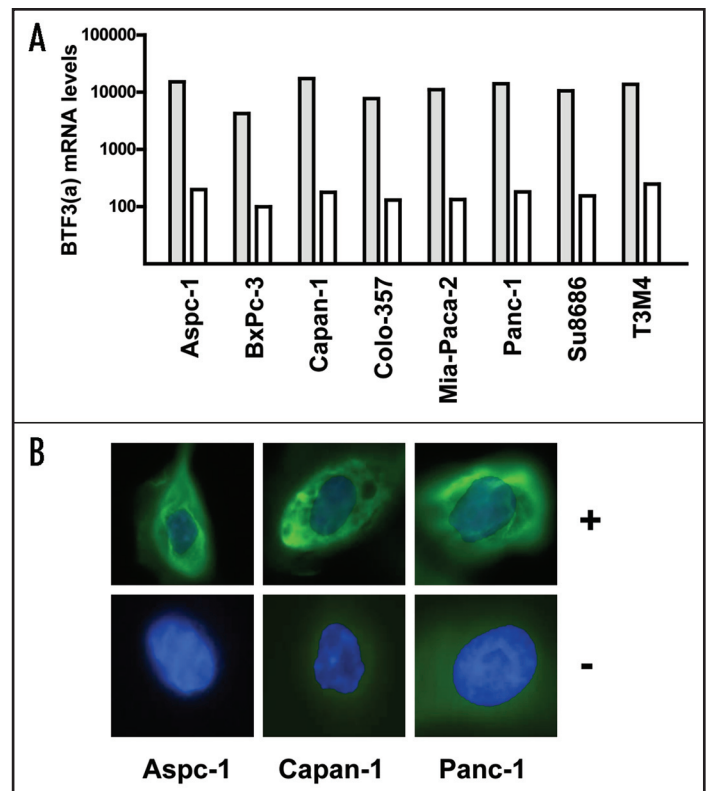


Figure 3. Expression and localization of BTF3 in pancreatic cancer cell lines. (A) Real-time quantitative RT-PCR analysis of total BTF3 (grey bars) and BTF3a (white bars) mRNA levels in pancreatic cancer cell lines was performed as described in the Methods section. RNA input was normalized to the average expression of the two housekeeping genes HPRT and cyclophilin B, and is presented as copy number/ $\mu$ l cDNA. (B) Immunofluorescence analysis was performed using polyclonal rabbit BTF3 antibodies (+) vs. control rabbit IgG (-). DAPI was used for nuclear counterstaining. Note the strong cytoplasmic and faint nuclear BTF3 staining in pancreatic cancer cells.

0.14–0.64) (Fig. 1C). However, there was no significant correlation between total BTF3 or BTF3a mRNA levels and different stages of PDAC.

**BTF3 localization in tubular complexes and pancreatic cancer cells.** In order to localize BTF3 in pancreatic tissues, immunohistochemistry was performed. The utilized antibody recognized both isoforms (BTF3a and BTF3b). In normal pancreatic tissues, weak to moderate BTF3 staining was detected in the cytoplasm and nuclei of acinar and ductal cells (Fig. 2A and 2B). In CP tissues, BTF3 was strongly localized in the cytoplasm and nuclei of tubular complexes, which are characteristic features of CP and PDAC tissues (Fig. 2C and 2D). In contrast, inflammatory cells, nerves, and blood vessels were devoid of BTF3 immunoreactivity (Fig. 2E). In PDAC tissues, intense staining of BTF3 was present in the cytoplasm and nuclei of cancer cells, as well as in tubular complexes (Fig. 2F–2H). The specificity of staining was verified using normal rabbit IgG in consecutive PDAC tissue sections (Fig. 2H and 2I).

**Silencing of BTF3 in human pancreatic cancer cell lines by siRNA transfection.** In the next set of experiments, total BTF3 and BTF3a mRNA and protein levels were determined in eight human pancreatic cancer cell lines by qRT-PCR, immunoblotting and immunofluorescence. Both isoforms were expressed in all tested pancreatic cancer cells. The highest total BTF3 mRNA levels (16569 copies/ $\mu$ l

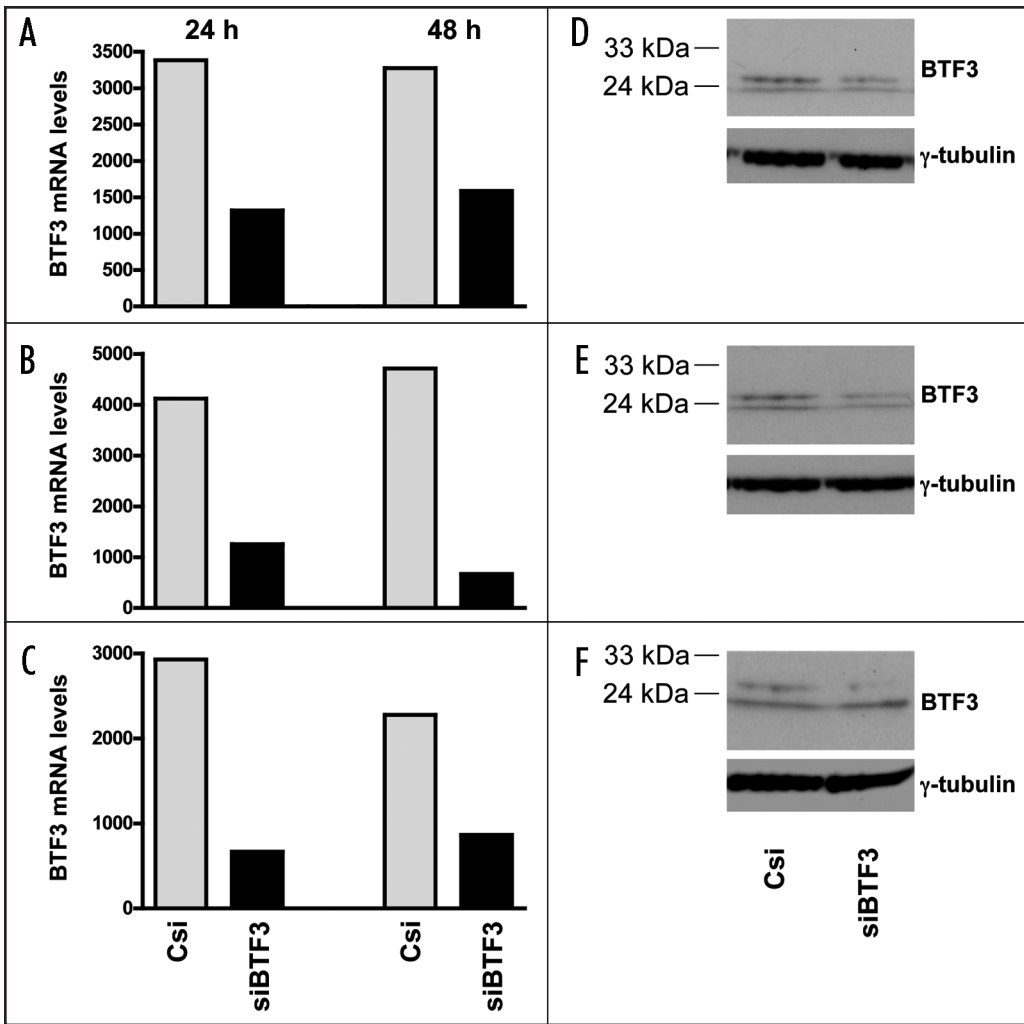
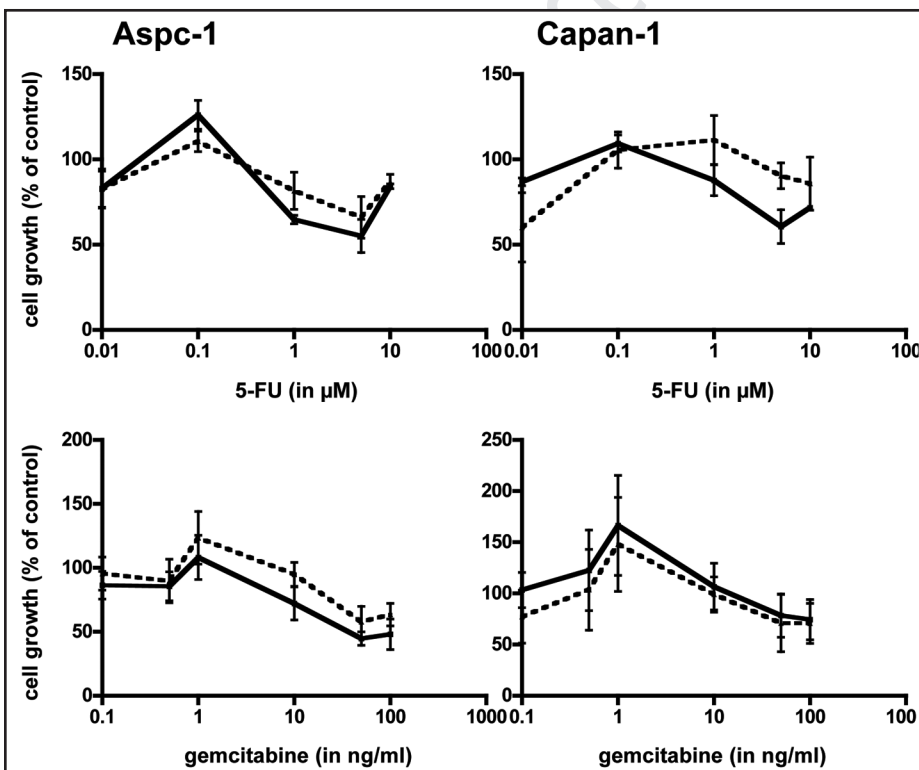


Figure 4. Effects of BTF3 siRNA transfection on BTF3 levels in human pancreatic cancer cells. Aspc-1 (A), Capan-1 (B) and Panc-1 (C) pancreatic cancer cell lines were transfected with BTF3 siRNA (black) or control siRNA (Csi) (grey) for the indicated time periods, and subjected to qRT-PCR analysis as described in the Methods section. Bars represent BTF3 mRNA copy number/ $\mu$ l cDNA. RNA input was normalized to the average expression of the two housekeeping genes HPRT and cyclophilin B. (D–F) Cell lysates from control siRNA transfected (Csi) or BTF3 siRNA transfected pancreatic cancer cell lines were subjected to immunoblot analysis using polyclonal rabbit BTF3 antibodies as described in the Methods section. BTF3a and BTF3b isoforms were detected as 27 and 22 kDa bands, respectively, in Aspc-1 (D), Capan-1 (E) and Panc-1 (F) pancreatic cancer cell lines.



cDNA) were observed in Capan-1 and the lowest (6580 copies/ $\mu$ l cDNA) in BxPc-3 pancreatic cancer cell lines (Fig. 3A). Similarly, BTF3a exhibited maximum mRNA levels of 320 copies/ $\mu$ l cDNA in T3M4 and a minimum of 74 copies/ $\mu$ l cDNA in BxPc-3 pancreatic cancer cells. Immunoblot analysis confirmed the qRT-PCR data, demonstrating BTF3 expression in Aspc-1, Capan-1 and Panc-1 pancreatic cancer cell lines at comparable levels. Specifically, two bands were detected at 22 and 27 kDa, representing BTF3b and BTF3a isoforms, respectively (data not shown). These results were further confirmed by immunofluorescence in Aspc-1, Capan-1, and Panc-1 cells, where BTF3 was predominantly localized in the cytoplasm with faint nuclear staining (Fig. 3B).

**Effects of BTF3 silencing on chemo- and radiosensitivity in pancreatic cancer cells.** To assess the functional role of BTF3, BTF3 mRNA silencing experiments were performed in 3 pancreatic cancer cell lines which expressed relative high BTF3 mRNA levels: Aspc-1, Capan-1 and Panc-1. The maximum BTF3 mRNA silencing effects after 24 and 48 h of

Figure 5. Impact of BTF3 silencing on the response of pancreatic cancer cells to chemotherapy. Aspc-1 (left) and Capan-1 (right) pancreatic cancer cells were transfected with BTF3 siRNA (continuous line) or control siRNA (interrupted line) and then exposed to increasing concentrations of 5-FU or gemcitabine as described in the Methods section. The decrease in cell growth is expressed as percentage of control cells. Results are presented as mean  $\pm$  SEM (standard error of the mean) of three independent experiments.

BTF3 siRNA treatment were 61% and 51.6% in Aspc-1 cells (Fig. 4A), 69.5% and 85.8% in Capan-1 cells (Fig. 4B) and 77.2% and 62% in Panc-1 cells (Fig. 4C), respectively. These results were confirmed by immunoblot analysis, demonstrating BTF3 down-regulation in the three cell lines after BTF3 silencing compared to control siRNA and non-transfected cells (Fig. 4D–F).

Since BTF3 has been suggested to play a role in apoptosis, we investigated the effects of BTF3 silencing on the responsiveness of Aspc-1 and Capan-1 pancreatic cancer cells to 5-FU and gemcitabine—two commonly used chemotherapeutic drugs—and  $\gamma$ -irradiation. As expected, both 5-FU and gemcitabine exhibited dose-dependent cytotoxic effects in Aspc-1 and Capan-1 cells. However, silencing of BTF3 mRNA did not significantly alter the chemosensitivity in either of the cell lines (Fig. 5). The effects of BTF3 silencing on the response to  $\gamma$ -irradiation (15 Gy) revealed significant G<sub>2</sub>/M phase cell cycle arrest in both Aspc-1 and Capan-1 cell lines in response to radiation (Fig. 6). However, silencing of BTF3 expression did not significantly alter the radiosensitivity in either cell line.

**Identification of transcriptional targets of BTF3 in pancreatic cancer cells.** Because BTF3 acts as a transcription factor,<sup>5</sup> Aspc-1, Capan-1 and Panc-1 pancreatic cancer cell lines were analyzed using DNA micro-array analysis following BTF3 silencing by siRNA. The expression of 3500 PDAC-related genes were compared between the silenced and control cells. Classification by correspondence analysis resulted in the formation of two distinct clusters for BTF3 and control siRNA-transfected Aspc-1 (Fig. 7A), Capan-1 (Fig. 7B) and Panc-1 (Fig. 7C) cells, and profiling the RNA produced a distinct blot position. All repetitions of the analysis produced the same result; actually forming a cluster in the correspondence analysis. Distances between clusters demonstrated that the sample exhibited a significantly different transcriptional profile. Figure 8 summarizes the significantly differentially expressed genes in control vs. BTF3 siRNA-transfected cells. For example, significant transcriptional regulation of ephrin receptor 2 (EPHB2) gene—among other genes—by BTF3 was observed in all three cell lines. EPHB2 mRNA exhibited 73%, 22%, and 64% reductions in response to BTF3 mRNA silencing in Aspc-1, Capan-1 and Panc-1 cells, respectively. These data were further validated by qRT-PCR, where BTF3 mRNA silencing led to 22.1%, 31.4%, and 30% reductions in EPHB2 mRNA levels in Aspc-1, Capan-1 and Panc-1 cells, respectively (Fig. 9A).

**EPHB2 expression and co-localization with BTF3 in pancreatic cancer.** Because EPHB2 is transcriptionally regulated by BTF3 in pancreatic cancer cells, qRT-PCR analysis was performed to correlate the mRNA levels of total BTF3, BTF3a and EPHB2 in a subgroup of normal pancreatic (n = 10) and PDAC (n = 32) tissues (Fig. 9B). This analysis revealed 2.7-fold increased median EPHB2 mRNA levels in PDAC compared to normal pancreatic tissues (p < 0.005). The median EPHB2 mRNA expression was 90 (range: 12–362) copies/ $\mu$ l cDNA in PDAC tissues, whereas the median

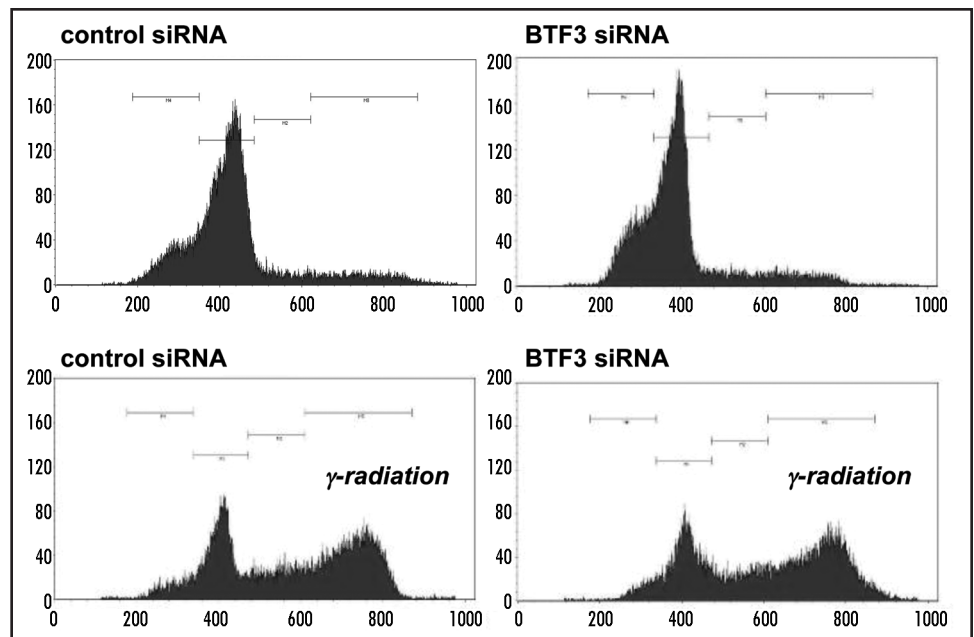


Figure 6. Impact of BTF3 silencing on the response of pancreatic cancer cells to radiotherapy. Aspc-1 pancreatic cancer cells were transfected with BTF3 siRNA or control siRNA as indicated and then exposed to irradiation 7.5 Gy/min for 2 min. Flow cytometry was carried out as described in the Methods section. Graphs represent data from one of three independent experiments.

total BTF3 mRNA was 34 (range: 0–88) copies/ $\mu$ l cDNA in normal pancreatic tissues. Interestingly, there was a significant up-regulation in the median mRNA expression levels of both EPHB2 and BTF3a, but not total BTF3, in the same group of PDAC tissues compared to normal pancreatic tissues. To further confirm the association of BTF3a and EPHB2 in PDAC tissues, immunohistochemistry for both BTF3 and EPHB2 was carried out next. This analysis demonstrated co-localization of both BTF3 and EPHB2 in the cytoplasm of pancreatic cancer cells and tubular complexes of PDAC cases (Fig. 9C and 9D).

## DISCUSSION

Transcription factors are frequently deregulated in PDAC, leading to different pathophysiological effects in this malignancy. For example, Id1 and Id2, which belong to the Id family of helix-loop-helix (HLH) proteins, are markedly overexpressed in pancreatic cancer cells and tubular complexes, leading to increased pancreatic cancer cell growth.<sup>26,27</sup> Other transcription factors, such as Smad2, Smad6, and Smad7, are overexpressed in PDAC, leading to deregulation of TGF- $\beta$  signaling, and thus enhancing the tumorigenicity of pancreatic cancer cells.<sup>19,27-29</sup> In the present study, total BTF3 and its active isoform BTF3a were found to be overexpressed in PDAC tissues compared to NP tissues. This was predominantly due to overexpression of BTF3a, as shown by an increased BTF3a/total BTF3 ratio in PDAC cases compared to controls. Interestingly, total BTF3 mRNA was much more abundant than the BTF3a isoform suggesting that BTF3b is the prominent isoform, despite a higher ratio of BTF3a/total BTF3 in cancer versus NP tissues. The relatively low proportion of the active isoform BTF3a is striking; however, it is currently not known whether this is specific for pancreatic tissues or a general phenomenon. Nonetheless, these findings suggest the specific involvement of BTF3a in the pathogenesis of PDAC. These data were further supported by the localization of BTF3 in the

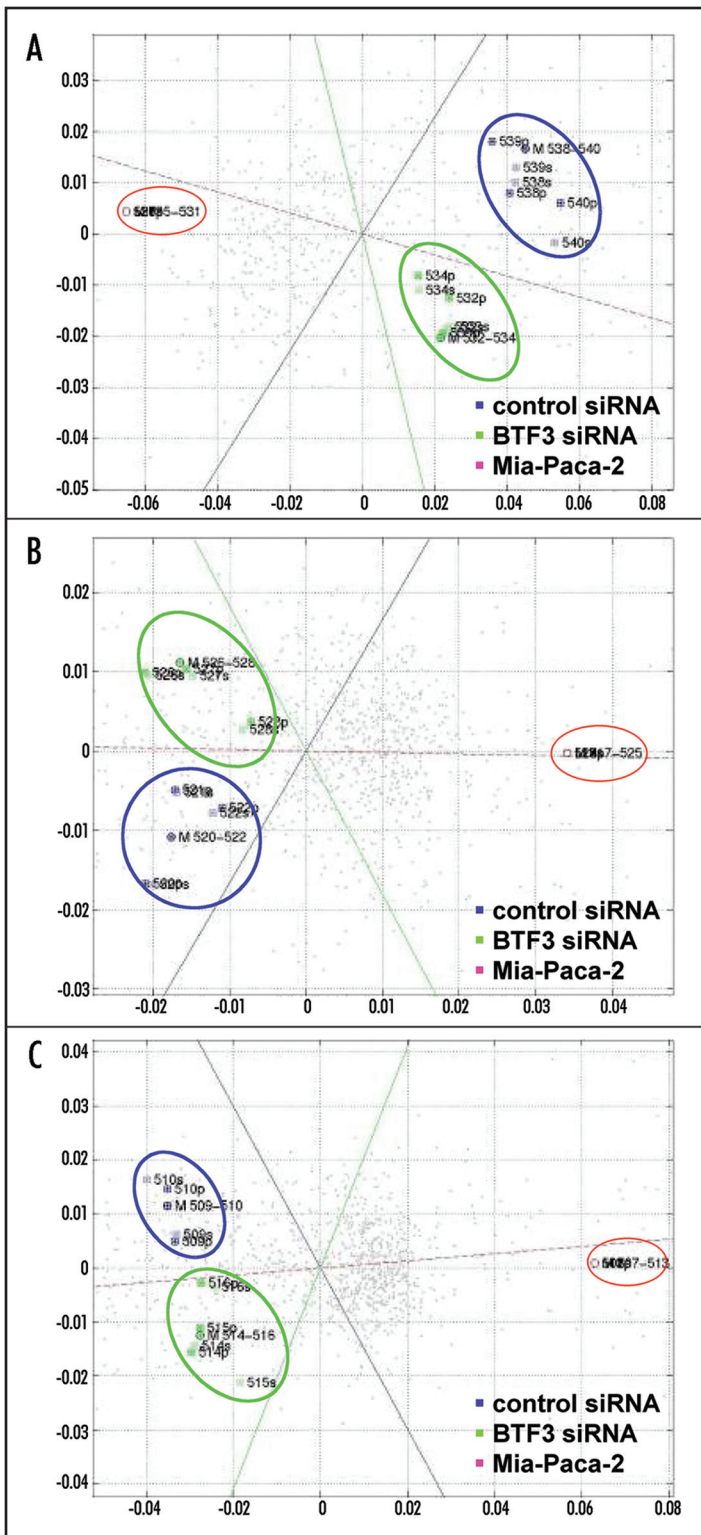


Figure 7 (Left). Correspondence cluster analysis. Aspc-1 (A), Capan-1 (B) and Panc-1 (C) pancreatic cancer cells were transfected with BTF3 siRNA or control siRNA. Total RNA was extracted and subjected to DNA array analysis as described in the Methods section. In the resulting biplot, each hybridization of the RNA from an individual tissue sample is depicted as a colored square. Each significantly differentially transcribed gene is shown as a black dot. Also, several guiding lines are displayed in the diagram. They correspond to the position of virtual genes whose transcription profiles would exhibit a signal under only one condition. Genes with insignificant changes are positioned close to the centroid of these lines, but are not shown in the blot. The samples from Aspc-1, Capan-1 and Panc-1 pancreatic cancer cells transfected with the BTF3 siRNA, control siRNA and wild type MiaPaCa-2 pancreatic cancer cells (as a reference control) form distinct clusters.

Aspc-1	Capan-1	Panc-1	mean	Gene
siRNA/control	siRNA/control	siRNA/control	siRNA/control	
0,47	0,32	0,49	0,42	ABL2
0,39	0,60	0,30	0,43	HPSE2
0,27	0,78	0,36	0,47	EPHB2
0,72	0,44	0,48	0,55	ATM
0,33	1,00	0,38	0,57	BAMBI
0,35	0,23	1,19	0,59	IMAGp958L10505Q2
0,48	0,37	0,95	0,60	ANXA2
0,91	0,46	0,46	0,61	HERC5
1,05	0,44	0,47	0,65	DAXX
0,49	1,03	0,47	0,66	RBL2
0,46	1,32	0,23	0,67	IMAGp998O145732Q2
1,16	0,44	0,47	0,69	YES1
0,37	1,55	0,17	0,70	DARS2
0,36	1,34	0,48	0,73	CST4
0,30	1,75	0,47	0,84	IMAGp998E20794Q2
0,47	1,00	3,30	1,59	GAS41
1,73	2,65	0,45	1,61	SSPN
2,56	2,05	0,88	1,83	NFKB2
2,37	2,04	1,10	1,84	MRV11
3,56	0,82	2,74	2,38	MADCAM1
2,61	4,15	0,93	2,57	RRAS2

Figure 8 (Above). Genes transcriptionally regulated by BTF3. Aspc-1, Capan-1 and Panc-1 pancreatic cancer cells were transfected with BTF3 or control siRNA. Total RNA was extracted and subjected to DNA array analysis as described in the Methods section. The mean gene expression was presented as a ratio of BTF3 siRNA and control siRNA from three independent experiments. Green = down-regulated genes (< 0.8-fold change), yellow = no change (0.8–1.2-fold change), red = up-regulation (≥ 1.2-fold change).

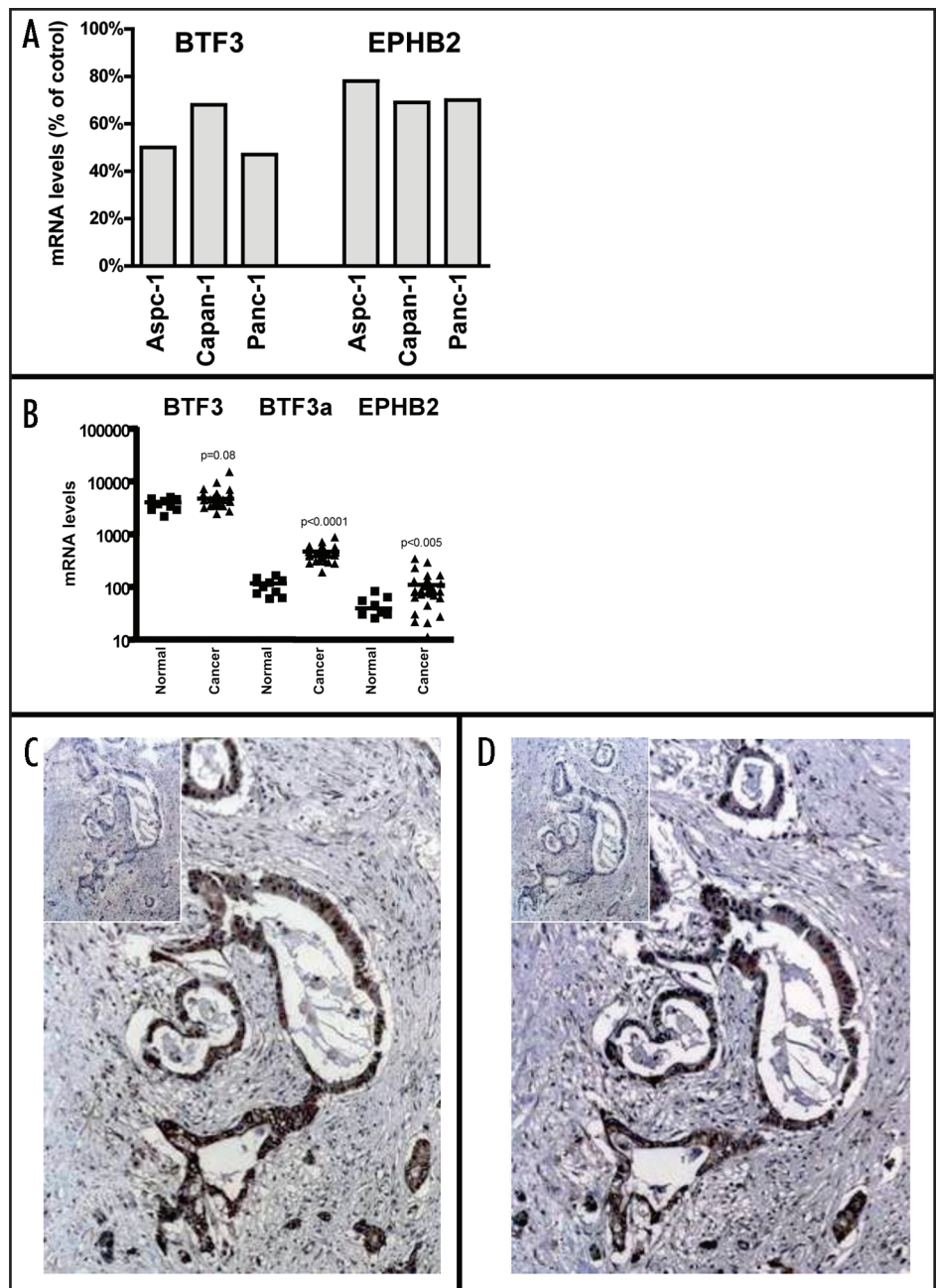
siRNA molecules did not result in significant changes in the sensitivity or resistance of Aspc-1 or Capan-1 cells to chemotherapeutic agents or radiotherapy, indicating that BTF3 does not directly influence cell apoptosis and/or cycle arrest in PDAC. It has been shown in other cancer cell types that downregulation of BTF3 is associated with apoptosis, suggesting that the ability of BTF3 to act as an anti-apoptotic factor is dependent on the type of cell or tissue.<sup>8–11</sup>

Analysis of the transcriptional activity of BTF3 has shown that BTF3 initiates the transcription process from proximal promoter elements such as the TATA box.<sup>5</sup> In the present study, BTF3 silencing led to decreased expression of a number of genes, most notably ephrin receptor B2 (EPHB2), V-ABL ablation murine leukemia viral oncogene homolog 2 (ABL2), heparanase 2 (HPSE2) and ataxia-telangectasia mutated gene (ATM).

tubular complexes of both CP and PDAC, in the cancer cells in PDAC, as well as in cultured pancreatic cancer cells, although it has to be emphasized that the used antibody recognizes both isoforms of BTF3.

PDAC frequently exhibits resistance to both chemotherapy and radiotherapy. The mechanisms of this resistance are not completely understood, but the combination of chemotherapy and radiotherapy with molecular therapy shows promising effects in treatment of PDAC.<sup>30,31</sup> In the current study, silencing of BTF3 using specific

Figure 9. Correlation analysis of BTF3 and EPHB2 in pancreatic cancer. (A) Validation of BTF3 and EPHB2 mRNA expression by qRT-PCR in pancreatic cancer cells. Aspc-1, Capan-1 and Panc-1 pancreatic cancer cells were transfected with BTF3 and control siRNA. RNA was extracted and qRT-PCR was performed as described in the Methods section. Bars represent the mRNA expression levels of BTF3 and EPHB2 as percent of control. (B) mRNA expression levels of BTF3, BTF3a and EPHB2 in a sub-group of normal and pancreatic cancer tissues: Real-time qRT-PCR analysis in normal (squares) and PDAC (triangles) tissue samples was performed as described in the Methods section. Horizontal lines represent the median mRNA levels. RNA input was normalized to the average expression of the two housekeeping genes HPRT and cyclophilin B. (C and D) Immunohistochemistry analysis was performed in consecutive PDAC tissue sections using BTF3 (C) and EPHB2 (D) antibodies demonstrating co-localization of both proteins in pancreatic cancer cells. Note the absent staining in consecutive tissue sections incubated with normal rabbit or goat IgG as negative controls (C and D, insets).



The structure of EPHB2 is similar to that of the ephrin receptor (EphA8), which lacks the TATA box in its putative promoter regions.<sup>32</sup> EPHB receptor protein tyrosine kinases are overexpressed in various tumors of the gastrointestinal tract, such as colorectal, esophagus, small intestine,<sup>33-35</sup> gastric and hepatocellular carcinomas.<sup>36</sup> EPHB2 is linked to the progression of gastric tumors,<sup>37</sup> and has been shown to regulate endothelial cell function.<sup>38</sup> In the present study, we have identified EPHB2 as a transcriptional target of BTF3 in pancreatic cancer cell lines and documented co-localization of both molecules in pancreatic cancer cells in vivo. These findings point to the importance of BTF3 in regulating the expression of signaling molecules that may be involved in the progression of PDAC.

In addition, BTF3 silencing led to decreased HPSE2 expression in pancreatic cancer cells. Members of the heparanase family are endo- $\beta$ -glucuronidases that degrade the heparan sulfate chains of proteoglycans in the cell membrane and extracellular matrix in many epithelial and mesenchymal malignant tissues.<sup>39-44</sup> They contain a TATA-less, GC-rich promoter region.<sup>45</sup> HPSE, which is closely related to HPSE2, is overexpressed in PDAC, and facilitates pancreatic cancer cell invasion,<sup>46</sup> indicating that BTF3 may act as a promoting factor for extracellular matrix degradation in PDAC.

Furthermore, the tyrosine kinase ABL2, an apoptosis-promoting factor that was first isolated from chronic myeloid leukemia cells,<sup>47</sup> is overexpressed in microdissected PDAC cells.<sup>48</sup> Apart from the growth-promoting effects of ABL2 in myeloid leukemia cells,<sup>47</sup> the exact function and signaling pathway of ABL2 in PDAC or other tumors are not known. Our data suggest that BTF3 might regulate ABL2 transcription in pancreatic cancer cells.

ATM, a protein kinase that is involved in DNA repair and/or cell

cycle control,<sup>49</sup> is thought to act as a tumor suppressor, and ATM mutations are associated with cancer development.<sup>50-53</sup> In PDAC, there is increased ATM expression,<sup>54</sup> although the functional consequences are not known.

On the other hand, silencing of BTF3 led to the induction of other genes, such as k-ras oncogene-associated gene (KRAG), related ras viral oncogene homolog (RRAS2), NF $\kappa$ B, murine retrovirus integration site 1 (MRV1) and mucosal vascular addressin cell adhesion molecule 1 (MADCAM1). These five genes are frequently associated with tumorigenesis. For example, KRAG is expressed in lung and ovarian carcinoma cells,<sup>55</sup> but its functional role has not been described in these tumors. RRAS2 is frequently overexpressed in squamous carcinoma cells<sup>56</sup> and in esophageal<sup>57</sup> and breast carcinomas.<sup>58,59</sup> Another factor, MRV1, regulates cellular calcium release,<sup>60</sup> and is frequently disturbed in pancreatic endocrine tumors.<sup>61,62</sup>

In addition, the nuclear transcription factor NF $\kappa$ B regulates the expression of a number of genes that are involved in tumorigenesis, and suppression of NF $\kappa$ B is associated with increased chemosensitivity as well as induction of apoptosis.<sup>63,64</sup> This indicates that BTF3 might influence cell growth through regulation of the expression of NF $\kappa$ B and its target genes in pancreatic cancer cells.

In conclusion, BTF3 is overexpressed in PDAC and has the potential to act as a positive or negative transcriptional regulator of genes involved in different pathophysiologic aspects of PDAC, such as epithelial/extracellular matrix degradation, cell growth, and cell cycle regulation.

## References

- Zheng XM, Moncollin V, Egly JM, Chambon P. A general transcription factor forms a stable complex with RNA polymerase B (II). *Cell* 1987; 50:361-8.
- Cavallini B, Faus I, Matthes H, Chipoulet JM, Winsor B, Egly JM, Chambon P. Cloning of the gene encoding the yeast protein BTF1Y, which can substitute for the human TATA box-binding factor. *Proc Natl Acad Sci USA* 1989; 86:9803-7.
- Cavallini B, Huet J, Plassat JL, Sentenac A, Egly JM, Chambon P. A yeast activity can substitute for the HeLa cell TATA box factor. *Nature* 1988; 334:77-80.
- Kanno M, Chalut C, Egly JM. Genomic structure of the putative BTF3 transcription factor. *Gene* 1992; 117:219-28.
- Zheng XM, Black D, Chambon P, Egly JM. Sequencing and expression of complementary DNA for the general transcription factor BTF3. *Nature* 1990; 344:556-9.
- Wynick D, Small CJ, Bacon A, Holmes FE, Norman M, Ormandy CJ, Kilic E, Kerr NC, Ghatei M, Talamantes F, Bloom SR, Pachnis V. Galanin regulates prolactin release and lactotroph proliferation. *Proc Natl Acad Sci USA* 1998; 95:12671-6.
- Deng JM, Behringer RR. An insertional mutation in the *BTF3* transcription factor gene leads to an early postimplantation lethality in mice. *Transgenic Res* 1995; 4:264-9.
- Bloss TA, Witze ES, Rothman JH. Suppression of CED-3-independent apoptosis by mitochondrial  $\beta$ NAC in *Caenorhabditis elegans*. *Nature* 2003; 424:1066-71.
- Brockstedt E, Otto A, Rickers A, Bommert K, Wittmann-Liebold B. Preparative high-resolution two-dimensional electrophoresis enables the identification of RNA polymerase B transcription factor 3 as an apoptosis-associated protein in the human BL60-2 Burkitt lymphoma cell line. *J Protein Chem* 1999; 18:225-31.
- Thiede B, Dimmler C, Siejak F, Rudel T. Predominant identification of RNA-binding proteins in Fas-induced apoptosis by proteome analysis. *J Biol Chem* 2001; 276:26044-50.
- Li R, Liu XL, Du QF, Zhang S, Luo RC, Zhou SY. Proteome analysis of apoptotic K562 cells induced by harringtonine. *Zhonghua Xue Ye Xue Za Zhi* 2004; 25:323-7.
- Ordreman F, Vindigni M, Gonzales ML, Nicolini B, Candiano G, Zanotti B, Skrap M, Pizzolito S, Stanta G, Vindigni A. Proteomic studies on low- and high-grade human brain astrocytomas. *J Proteome Res* 2005; 4:698-708.
- Duncan DS, McWilliam P, Tighe O, Parle-McDermott A, Croke DT. Gene expression differences between the microsatellite instability (MIN) and chromosomal instability (CIN) phenotypes in colorectal cancer revealed by high-density cDNA array hybridization. *Oncogene* 2002; 21:3253-7.
- Friess H, Ding J, Kleeff J, Fenkel L, Rosinski JA, Guweidhi A, Reidhaar-Olson JF, Korc M, Hammer J, Buchler MW. Microarray-based identification of differentially expressed growth- and metastasis-associated genes in pancreatic cancer. *Cell Mol Life Sci* 2003; 60:1180-99.
- Friess H, Ding J, Kleeff J, Liao Q, Berberat PO, Hammer J, Buchler MW. Identification of disease-specific genes in chronic pancreatitis using DNA array technology. *Ann Surg* 2001; 234:769-78, (discussion 78-9).
- Guo J, Kleeff J, Li J, Ding J, Hammer J, Zhao Y, Giese T, Korc M, Buchler MW, Friess H. Expression and functional significance of CDC25B in human pancreatic ductal adenocarcinoma. *Oncogene* 2004; 23:71-81.
- Kayed H, Kleeff J, Keleg S, Guo J, Ketterer K, Berberat PO, Giese N, Esposito I, Giese T, Buchler MW, Friess H. Indian hedgehog signaling pathway: Expression and regulation in pancreatic cancer. *Int J Cancer* 2004; 110:668-76.
- Guo DL, Zhang J, Yuen ST, Tsui WY, Chan AS, Ho C, Ji J, Leung SY, Chen X. Reduced expression of EphB2 that parallels invasion and metastasis in colorectal tumours. *Carcinogenesis* 2006; 27:454-64.
- Kleeff J, Ishiwata T, Maruyama H, Friess H, Truong P, Buchler MW, Falb D, Korc M. The TGF- $\beta$  signaling inhibitor Smad7 enhances tumorigenicity in pancreatic cancer. *Oncogene* 1999; 18:5363-72.
- Esposito I, Bauer A, Hoheisel JD, Kleeff J, Friess H, Bergmann F, Rieker RJ, Otto HF, Kloppel G, Penzel R. Microcystic tubulopapillary carcinoma of the pancreas: A new tumor entity? *Virchows Arch* 2004; 444:447-53.
- Korc M, Chandrasekar B, Yamanaka Y, Friess H, Buchler M, Beger HG. Overexpression of the epidermal growth factor receptor in human pancreatic cancer is associated with concomitant increases in the levels of epidermal growth factor and transforming growth factor  $\alpha$ . *J Clin Invest* 1992; 90:1352-60.
- Fellenberg K, Hauser NC, Brors B, Neutzner A, Hoheisel JD, Vingron M. Correspondence analysis applied to microarray data. *Proc Natl Acad Sci USA* 2001; 98:10781-6.
- Fellenberg K, Hauser NC, Brors B, Hoheisel JD, Vingron M. Microarray data warehouse allowing for inclusion of experiment annotations in statistical analysis. *Bioinformatics* 2002; 18:423-33.
- Beissbarth T, Fellenberg K, Brors B, Arribas-Prat R, Boer J, Hauser NC, Scheideler M, Hoheisel JD, Schutz G, Poustka A, Vingron M. Processing and quality control of DNA array hybridization data. *Bioinformatics* 2000; 16:1014-22.
- Brazma A, Hingamp P, Quackenbush J, Sherlock G, Spellman P, Stoeckert C, Aach J, Ansorge W, Ball CA, Causton HC, Gaasterland T, Glenissov P, Holstege FC, Kim IF, Markowitz V, Matese JC, Parkinson H, Robinson A, Sarkans U, Schulze-Kremer S, Stewart J, Taylor R, Vilo J, Vingron M. Minimum information about a microarray experiment (MIAME)-toward standards for microarray data. *Nat Genet* 2001; 29:365-71.
- Kleeff J, Ishiwata T, Friess H, Buchler MW, Israel MA, Korc M. The helix-loop-helix protein Id2 is overexpressed in human pancreatic cancer. *Cancer Res* 1998; 58:3769-72.
- Maruyama H, Kleeff J, Wildi S, Friess H, Buchler MW, Israel MA, Korc M. Id-1 and Id-2 are overexpressed in pancreatic cancer and in dysplastic lesions in chronic pancreatitis. *Am J Pathol* 1999; 155:815-22.
- Kleeff J, Friess H, Simon P, Susmallian S, Buchler P, Zimmermann A, Buchler MW, Korc M. Overexpression of Smad2 and co-localization with TGF- $\beta$ 1 in human pancreatic cancer. *Dig Dis Sci* 1999; 44:1793-802.
- Kleeff J, Maruyama H, Friess H, Buchler MW, Falb D, Korc M. Smad6 suppresses TGF- $\beta$ -induced growth inhibition in COLO-357 pancreatic cancer cells and is overexpressed in pancreatic cancer. *Biochem Biophys Res Commun* 1999; 255:268-73.
- Yokoi K, Sasaki T, Bucana CD, Fan D, Baker CH, Kitada Y, Kuwai T, Abbruzzese JL, Fidler IJ. Simultaneous inhibition of EGFR, VEGFR, and platelet-derived growth factor receptor signaling combined with gemcitabine produces therapy of human pancreatic carcinoma and prolongs survival in an orthotopic nude mouse model. *Cancer Res* 2005; 65:10371-80.
- Tang PA, Tsao MS, Moore MJ. A review of erlotinib and its clinical use. *Expert Opin Pharmacother* 2006; 7:177-93.
- Jeong J, Choi S, Gu C, Lee H, Park S. Genomic structure and promoter analysis of the mouse *EphA8* receptor tyrosine kinase gene. *DNA Cell Biol* 2000; 19:291-300.
- Liu W, Ahmad SA, Jung YD, Reinmuth N, Fan F, Bucana CD, Ellis LM. Coexpression of ephrin-Bs and their receptors in colon carcinoma. *Cancer* 2002; 94:934-9.
- Lugli A, Spichtin H, Maurer R, Mirlacher M, Kiefer J, Huusko P, Azorsa D, Terracciano L, Sauter G, Kallioniemi OP, Mousseis S, Tornillo L. EphB2 expression across 138 human tumor types in a tissue microarray: High levels of expression in gastrointestinal cancers. *Clin Cancer Res* 2005; 11:6450-8.
- Kataoka H, Tanaka M, Kanamori M, Yoshii S, Ihara M, Wang YJ, Song JP, Li ZY, Arai H, Otsuki Y, Kobayashi T, Konno H, Hanai H, Sugimura H. Expression profile of EFNB1, EFNB2, two ligands of EPHB2 in human gastric cancer. *J Cancer Res Clin Oncol* 2002; 128:343-8.
- Hafner C, Schmitz G, Meyer S, Bataille F, Hau P, Langmann T, Dietmaier W, Landthaler M, Vogt T. Differential gene expression of *Eph* receptors and ephrins in benign human tissues and cancers. *Clin Chem* 2004; 50:490-9.
- Davalos V, Dopeso H, Velho S, Ferreira AM, Cirnes L, Diaz-Chico N, Bilbao C, Ramirez R, Rodriguez G, Falcon O, Leon L, Niessen RC, Keller G, Dallenbach-Hellweg G, Espin E, Armengol M, Plaja A, Perucho M, Imai K, Yamamoto H, Geberth JF, Diaz-Chico JC, Hofstra RM, Woerner SM, Seruca R, Schwartz S, Arango D. High *EPHB2* mutation rate in gastric but not endometrial tumors with microsatellite instability. *Oncogene* 2006.
- Salvucci O, Sierra MD, Martina JA, McCormick PJ, Tosato G. EphB2 and EphB4 receptors forward signaling promotes SDF-1-induced endothelial cell chemotaxis and branching remodeling. *Blood* 2006.
- Chambers AF, Matrisian LM. Changing views of the role of matrix metalloproteinases in metastasis. *J Natl Cancer Inst* 1997; 89:1260-70.
- Fidler IJ, Radinsky R. Search for genes that suppress cancer metastasis. *J Natl Cancer Inst* 1996; 88:1700-3.
- Fidler IJ. Critical determinants of cancer metastasis: Rationale for therapy. *Cancer Chemother Pharmacol* 1999; 43(Suppl):S3-10.
- Nakajima M, Irimura T, Nicolson GL. A solid-phase substrate of heparanase: Its application to assay of human melanoma for heparan sulfate degradative activity. *Anal Biochem* 1986; 157:162-71.
- Nakajima M, Irimura T, Nicolson GL. Tumor metastasis-associated heparanase (heparan sulfate endoglycosidase) activity in human melanoma cells. *Cancer Lett* 1986; 31:277-83.
- Xiao Y, Kleeff J, Shi X, Buchler MW, Friess H. Heparanase expression in hepatocellular carcinoma and the cirrhotic liver. *Hepatology* 2003; 26:192-8.
- Jiang P, Kumar A, Parrillo JE, Dempsey LA, Platt JL, Prinz RA, Xu X. Cloning and characterization of the human heparanase-1 (*HPR1*) gene promoter: Role of GA-binding protein and Sp1 in regulating HPR1 basal promoter activity. *J Biol Chem* 2002; 277:9899-98.
- Koliopoulos A, Friess H, Kleeff J, Shi X, Liao Q, Pecker I, Vlodavsky I, Zimmermann A, Buchler MW. Heparanase expression in primary and metastatic pancreatic cancer. *Cancer Res* 2001; 61:4655-9.
- Cong XL, Li B, Yang RC, Feng SZ, Chen SJ, Han ZC. Enhanced growth suppression of Philadelphia1 leukemia cells by targeting bcr3/abl2 and VEGF through antisense strategy. *Leukemia* 2005; 19:1517-24.
- Crnogorac-Jurcovic T, Efthimiou E, Nielsen T, Loader J, Terris B, Stamp G, Baron A, Scarpa A, Lemoine NR. Expression profiling of microdissected pancreatic adenocarcinomas. *Oncogene* 2002; 21:4587-94.
- Lavin MF, Birrell G, Chen P, Kozlov S, Scott S, Gueven N. ATM signaling and genomic stability in response to DNA damage. *Mutat Res* 2005; 569:123-32.

50. Vorechovsky I, Rasio D, Luo L, Monaco C, Hammarstrom L, Webster AD, Zaloudik J, Barbanti-Brodani G, James M, Russo G, et al. The *ATM* gene and susceptibility to breast cancer: Analysis of 38 breast tumors reveals no evidence for mutation. *Cancer Res* 1996; 56:2726-32.
51. Vorechovsky I, Luo L, Lindblom A, Negrini M, Webster AD, Croce CM, Hammarstrom L. *ATM* mutations in cancer families. *Cancer Res* 1996; 56:4130-3.
52. Morgan SE, Kastan MB. p53 and ATM: Cell cycle, cell death, and cancer. *Adv Cancer Res* 1997; 71:1-25.
53. Oliveira AM, Ross JS, Fletcher JA. **Tumor suppressor genes in breast cancer: The gatekeepers and the caretakers.** *Am J Clin Pathol* 2005; 124(Suppl):S16-2).
54. Yu G, Zhu MH, Zhu Z, Ni CR, Zheng JM, Li FM. Expression of ATM protein and its relationship with p53 in pancreatic carcinoma with tissue array. *Pancreas* 2004; 28:421-6.
55. Heighway J, Betticher DC, Hoban PR, Altermatt HJ, Cowen R. Coamplification in tumors of *KRAS2*, type 2 inositol 1,4,5 triphosphate receptor gene, and a novel human gene, *KRAG*. *Genomics* 1996; 35:207-14.
56. Arora S, Matta A, Shukla NK, Deo SV, Ralhan R. Identification of differentially expressed genes in oral squamous cell carcinoma. *Mol Carcinog* 2005; 42:97-108.
57. Sharma R, Sud N, Chattopadhyay TK, Ralhan R. TC21/R-Ras2 upregulation in esophageal tumorigenesis: Potential diagnostic implications. *Oncology* 2005; 69:10-8.
58. Clark GJ, Kinch MS, Gilmer TM, Burridge K, Der CJ. Overexpression of the Ras-related TC21/R-Ras2 protein may contribute to the development of human breast cancers. *Oncogene* 1996; 12:169-76.
59. Barker KT, Crompton MR. Ras-related *TC21* is activated by mutation in a breast cancer cell line, but infrequently in breast carcinomas in vivo. *Br J Cancer* 1998; 78:296-300.
60. Schlossmann J, Ammendola A, Ashman K, Zong X, Huber A, Neubauer G, Wang GX, Allescher HD, Korth M, Wilm M, Hofmann F, Ruth P. Regulation of intracellular calcium by a signalling complex of IRAG, IP3 receptor and cGMP kinase  $\beta$ . *Nature* 2000; 404:197-201.
61. Imamura M. Pancreatic endocrine tumor-from clinic to calcium sensing receptor. *Hum Cell* 2000; 13:65-9.
62. Yamamoto M, Nakano S, Mugikura M, Tachibana I, Ogami Y, Otsuki M. Pancreatic cancer and hypercalcemia associated with von Recklinghausen's disease. *J Gastroenterol* 1996; 31:728-31.
63. Garg A, Aggarwal BB. **Nuclear transcription factor-kappaB as a target for cancer drug development.** *Leukemia* 2002; 16:1053-68.
64. Shishodia S, Aggarwal BB. Cyclooxygenase (COX)-2 inhibitor celecoxib abrogates activation of cigarette smoke-induced nuclear factor (NF)-kappaB by suppressing activation of I $\kappa$ B kinase in human nonsmall cell lung carcinoma: Correlation with suppression of cyclin D1, COX-2, and matrix metalloproteinase-9. *Cancer Res* 2004; 64:5004-12.

ACCEPTED FOR PUBLICATION. DO NOT DISTRIBUTE.